Controllable Synthesis of Conducting Polypyrrole Nanostructures

Xuetong Zhang,*,†,‡ Jin Zhang,*,† Wenhui Song,‡ and Zhongfan Liu†

Key Laboratory for the Physics and Chemistry of Nanodevices, Centre for Nanoscale Science and Technology, College of Chemistry and Molecular Engineering, Peking University, Beijing 100871, P.R. China, and Wolfson Centre for Materials Processing, Brunel University, West London, UB8 3PH, United Kingdom

Received: August 4, 2005; In Final Form: October 7, 2005

Wire-, ribbon-, and sphere-like nanostructures of polypyrrole have been synthesized by solution chemistry methods in the presence of various surfactants (anionic, cationic, or nonionic surfactant) with various oxidizing agents [ammonium persulfate (APS) or ferric chloride ($FeCl_3$), respectively]. The surfactants and oxidizing agents used in this study have played a key role in tailoring the nanostructures of polypyrrole during the polymerization. It is inferred that the lamellar structures of a mesophase are formed by self-assembly between the cations of a long chain cationic surfactant [cetyltrimethylammonium bromide (CTAB) or dodeyltrimethylammonium bromide (DTAB)] and anions of oxidizing agent APS. These layered mesostructures are presumed to act as templates for the formation of wire- and ribbon-like polypyrrole nanostructures. In contrast, if a short chain cationic surfactant octyltrimethylammonium bromide (OTAB) or nonionic surfactant poly(ethylene glycol) mono-*p*-nonylphenyl ether (Oπ-10) is used, sphere-like polypyrrole nanostructures are obtained, whichever of the oxidizing agents mentioned above is used. In this case, micelles resulting from self-assembly among surfactant molecules are envisaged to serve as the templates while the polymerization happens. It is also noted that, if anionic surfactant sodium dodeyl surfate (SDS) is used, no characteristic nanostructures of polypyrrole were observed. This may be attributed to the doping effect of anionic surfactants into the resulting polypyrrole chains, and as a result, micelles self-assembled among surfactant molecules are broken down during the polymerization. The effects of monomer concentration, surfactant concentration, and surfactant chain length on the morphologies of the resulting polypyrrole have been investigated in detail. The molecular structures, composition, and electrical properties of the nanostructured polypyrrole have also been investigated in this study.

Introduction

Micrometer- or nanometer-sized conducting polymers have attracted great attention mainly due to their potential applications in electronic circuits, chemical and electrochemical sensors, photovoltaic cells, electrochromic devices, and field emission applications.[1−5] One of the key strategies for synthesizing conducting polymers with dimensions at such small scales is a template-directed synthesis.[6−12] Templates used in this route can be classified into two major categories, namely "hard" and "soft" templates. Hard templates, pioneered by Wu[6] and Martin,[7] include many kinds of conventional hard porous materials, such as porous aluminosilicate MCM-41[6] and microporous polymeric filtration membranes.[10] Recently hard templates have been extended to carbon nanotubes,[13] lipid tubule edges,[14] and electrospun polymer fibers[15] for synthesizing micrometer-/nanometer-sized conducting polymers. However, to obtain appropriate hard-template materials, scientists have to purchase or prepare appropriate porous materials before synthesizing the prospective materials. Moreover, to get pure conducting polymers, the hard-template materials have to be removed after the synthesis. This is very difficult in most cases, and may drastically alter or even destroy the resulting materials during recovery from the templates. On the other hand, soft-templates or molecule templates are often long range ordered structure self-assembled from certain surfactants or block copolymers, etc., which provide well-defined rooms or channels for conducting polymer chains to grow into micrometer-/nanometer-sized products.[16−18] The advantage of using these soft-template materials is that they are easy to remove after the synthesis, and in the meantime, the micro-/nanostructures of the resulting polymers can remain. Recently some novel template molecules including lipid[9] and cyclodextrin[19] have emerged. Moreover, surface micelles,[8,20] liquid-crystalline phases,[21,22] and extraneous electrical fields[22] have also been employed during the synthesis of conducting polymers. Various micrometer-/nanometer-sized conducting polymers have been synthesized with diverse molecule assemblies as the templates. For example, submicrometer-sized tube junctions and dendrites of polyaniline,[23] helical poly(ethylenedioxythiophene),[9] ribbon-like poly(*p*-phenylene vinylene),[24] etc., have been synthesized successfully, and even conducting polymer microcontainers with bowl-, cup-, or bottle-like morphologies have been generated electrochemically by a so-called "soap bubble" technique.[25,26]

Out of the curiosity of the previous finding of polypyrrole nanowire/robbins in the system of pyrrole/CTAB/APS,[27] herein we report a systematic study on the controllable synthesis of conducting polypyrrole nanostructures by using a variety of self-assembled surfactants as templates. Nanowire- and nanoribbon-like polypyrrole can be synthesized in the presence of long chain cationic surfactants [cetyltrimethylammonium bromide (CTAB) or dodeyltrimethylammonium bromide (DTAB)] and anions of

* Address correspondence to this author. Phone: 44-1895-267055. Fax: 44-1895-269737. E-mail: xuetong.zhang@brunel.ac.uk (Dr. X. Zhang) and jinzhang@pku.edu.cn (Dr. J. Zhang).
† Peking University.
‡ Brunel University.

10.1021/jp054335k CCC: $33.50
Published on Web 12/24/2005

the oxidizing agent of ammonium persulfate (APS). In the case of using the short chain cationic surfactant octyltrimethylammonium bromide (OTAB) or the nonionic surfactant poly(ethylene glycol) mono-*p*-nonylphenyl ether (Oπ-10) instead, regardless of the oxidizing agent used, nanosphere-like polypyrrole can be formed. However when the anionic surfactant sodium dodeyl sulfate (SDS) is used, no characteristic nanofeature can be observed in the resulting products. The effects of surfactant concentration, surfactant chain length, monomer concentration, etc. on the morphologies of the resulting polypyrrole have been investigated in detail. The mechanisms of templates during the polymerization have been discussed. The molecular structures, composition, and electrical properties of the nanostructured polypyrrole have been investigated as well.

Experimental Section

The majority of the chemicals including pyrrole monomer, surfactants (CTAB, SDS, and Oπ-10), and oxidizing agents (APS and $FeCl_3$) were purchased from Beijing Chemical Reagents Company, with their purity in analytical grade except for Oπ-10 (average EO unit $n = 10$, chemical grade). Other surfactants, DTAB ($\cong$99%) and OTAB ($\geq$98%), were purchased from Sigma-Aldrich Company Ltd. Pyrrole monomer was purified by distillation before use. Other reagents were used as received without further purification.

The polypyrrole in the form of various nanostructures was synthesized by the solution chemistry method. The synthetic process was as follows: pyrrole monomers with a definite volume were added into a quantitative cationic (CTAB, DTAB, OTAB), anionic (SDS), or nonionic surfactant (Oπ-10) aqueous solution, respectively. Then an oxidizing agent (either APS or $FeCl_3$) aqueous solution was added into the above mixture to initiate the polymerization. When using APS as oxidizing agent, the monomer and the oxidizing agent were kept equal (1:1); however, when $FeCl_3$ was used as the oxidizing agent, the mole ratio of monomer to oxidizing agent was kept at 1:2. All solutions were precooled to 0$-$5 °C, and the polymerization in the final mixture went on at 0$-$5 °C for 24 h. After reaction, the precipitates were filtrated and washed with deionized water and ethanol alternately at least 3 times, then left to dry, resulting in a black powder.

The concentrations of the surfactant aqueous solutions used in the reaction systems were controlled in the ranges of micelle aggregations according to the literature, with a maximum of 12 cmc (critical micelle concentration) for the ionic surfactants. The cmc of CTAB is 0.87 mM in deionized water at room temperature and a transition from spherical to cylindrical micelles occurs at a concentration of more than 12 cmc at room temperature.[28,29] The cmcs for DTAB and OTAB are 14 mM and 0.9 M, respectively.[30,31] The cmc for SDS is 8.2 mM in deionized water at room temperature,[32] and its phase diagram was reported by Burducea.[33] Nonionic surfactant Oπ-10 is a derivative of the well-studied Triton X-100 with the same average number of EO and a slightly longer alkyl tail (three more CH_2). Although the full information on the properties of Oπ-10 aqueous solution is not available, it is certain that the concentration range of micelle aggregation for Oπ-10 (5 wt % used in the work) should be more or less similar to that for Triton X-100 (with the oblate micelles existing up to the concentration of 15 wt %[34]).

Scanning electron microscope (SEM) images were obtained at 10 kV with an XL30S-FEG field-emission instrument. High-resolution transmission electron microscope (HRTEM) images were recorded on a Tecnai F30 at 300 kV. Samples for both SEM and TEM were prepared by placing a drop of an aqueous suspension of polypyrrole onto a silicon wafer and carbon-coated copper grid, respectively. Infrared spectra were recorded with a Magna-IR 750 system using powdered samples. XPS analysis was performed with an Axis Ultra spectrometer (Kratos, UK) using Monochromatic Al Kα (1486.71 eV) radiation at 225 W power (15 mA, 15 kV). To compensate for surface charge effects, binding energies were calibrated by using the C1s hydrocarbon peak at 284.8 eV. Electrical conductivity was measured with an automatic computer controlled Keithley 220-programmable current source and 181-nanovoltmeter. Samples used for DC electrical-conductivity measurements were in the form of compressed pellets (12 mm in diameter and about 0.1 mm in thickness) obtained by applying a hydraulic pressure of about 10 MPa.

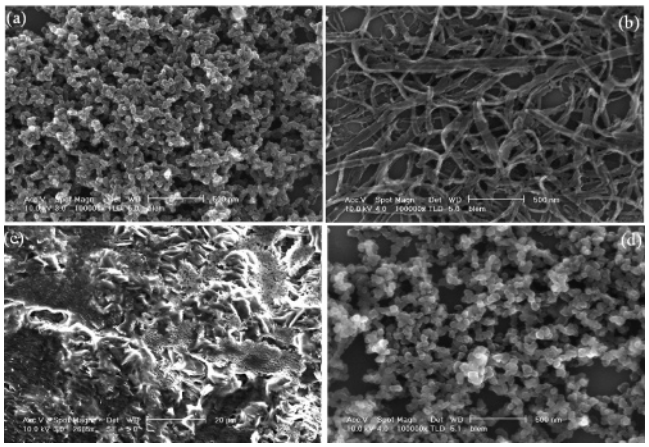

Figure 1. SEM images of polypyrrole nanostructures with different morphologies obtained by the different synthetic conditions (monomer concentration 15 mM): (a) sphere-like polypyrrole by using CTAB surfactant and $FeCl_3$ oxidizing agent; (b) ribbon-like polypyrrole by using CTAB surfactant and APS oxidizing agent; (c) no polypyrrole nanostructures were obtained by using SDS surfactant and APS oxidizing agent; and (d) sphere-like polypyrrole by using poly(ethylene glycol) mono-*p*-nonylphenyl ether (Oπ-10) surfactant and APS oxidizing agent.

TABLE 1: The Morphologies of the Resulting Polypyrrole Obtained in the Synthetic Conditions of Different Surfactants and Oxidizing Agents

polypyrrole nanostructures	surfactants				
	CTAB	DTAB	OTAB	Oπ-10	SDS
oxidizing agents					
APS	ribbon-like or wire-like		sphere-like		no geometrical nanofeature
$FeCl_3$	sphere-like				

Results and Discussion

Morphology of Polypyrrole. Table 1 summarizes the morphologies of the resulting polypyrrole obtained respectively in the synthetic conditions of different surfactants and oxidizing agents. To compare the effects of surfactant and oxidizing agents on the morphologies of the resulting polypyrrole nanostructures, the monomer concentrations were kept the same at 15 mM, and the resulting polypyrrole morphologies obtained in the synthetic conditions of different surfactants and oxidization agents are shown in Figure 1. In the case of using CTAB as a surfactant and keeping its concentration at 12 cmc, the different nanostructures of polypyrrole were obtained by using different oxidizing agents (Figure 1a,b). If the oxidizing agent $FeCl_3$ was

used, polypyrrole nanoparticles were formed, showing uniform sphere-like morphology with diameters in a narrow range between 35 and 60 nm (Figure 1a). However, if the oxidizing agent APS was used instead, the polypyrrole appeared to grow in the shape of ribbon-like nanostructures with widths in the range between 25 and 85 nm, heights in the range of several nanometers, and lengths up to several micrometers (Figure 1b). These indicate that the anions of the oxidizing agents may have played a different role of counterions of altering ion pair interaction and thus the CTAB packing parameter. In turn the growth of polypyrrole nanostructures has been confined in different ways during polymerization, providing a potential route to control the morphology of the resulting polypyrrole. There will be more discussions in the following sections.

The surfactant effects on the morphologies of the polypyrrole were also investigated by using other surfactants. When nonionic surfactant Oπ-10 (its concentration kept at 5 wt %) replaced the CTAB, whichever oxidizing agent ($FeCl_3$ and APS) was used, only nanosphere-like polypyrroles were obtained (Figure 1d shows an example of polypyrrole nanoparticles formed in the presence of oxidizing agent APS). The diameters of the nanospheres were in the range between 45 and 70 nm. However when anionic surfactant SDS (its concentration kept at 12 cmc) replaced the CTAB, in the presence of either oxidizing agent $FeCl_3$ or APS, no regular nanostructure of polypyrrole was observed (Figure 1c shows the morphology of polypyrrole formed in the case of using SDS and APS). In contrast with other surfactants, the surfactant SDS was difficult to remove completely. In consequence, the morphology shown in Figure 1c is actually the structure of the resulting polypyrrole mixed with SDS residue. These above observations indicate that, apart from the oxidizing agents, the surfactants can also have a significant influence on the formation of the polypyrrole morphology during polymerization.

What is the mechanism for determining the morphology of the polypyrrole behind the various and unpredictable factors in the reactions, such as the chemical structures of oxidizing agents and surfactants studied above, as well as the concentrations of monomer, oxidizing agents, and surfactants, etc.? Bearing this question in mind, we have some clear clues from the review of the fundamental knowledge, recent application of the self-assembly of surfactants,[20−22] and our previous results.[27] It is well established that surfactants assemble into micelles, spherical, oblate, or cylindrical structures, due to their amphiphilic nature in aqueous solution above a critical concentration. Further increases in the concentration result in the self-organization of micelles into periodic hexagonal, cubic, or lamellar mesophases. Recently, these self-assembly structures have been widely used as effective templates for synthesizing organic/inorganic/metal nanomaterials.[20−22,35−36] To be specific, when nonionic surfactant Oπ-10 was used, in the presence of either oxidizing agent $FeCl_3$ or APS, we supposed that amphiphilic macromolecular chains of Oπ-10 (5 wt %) self-assembled into sphere-like micelles without interference from the ionic oxidizing agent. The sphere-like micelles spatially separated and organized hydrophobic pyrrole monomers into the micelles through hydrophobic interaction. It should be pointed out that, even though pyrrole is soluble in water (0.9 M), it could easily enter the interior of the micelles. Such "hydrophobic" behaviors of pyrrole molecules in the micelle aggregation have already been reported by others.[8,20] Very recently, Manohar et al.[37] has further characterized that there is a small increase of hydrodynamic radius of micelles and a decrease of cmc after adding the pyrrole into the CTAB/water system.

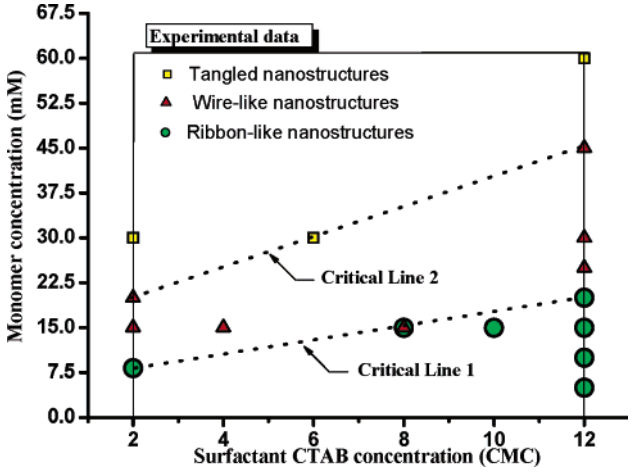

Figure 2. Threshold pyrrole concentrations for the nanostructure of resulting polypyrrole versus the surfactant concentration in the system of pyrrole/CTAB/APS. In the area below Critical Line 1, ribbon-like nanostructures would be synthesized, and in the area between Critical Line 1 and 2, wire-like nanostructures would be formed. Above Critical Line 2, highly entangled wire-like nanostructures and irregular structure of polypyrrole would appear.

After adding ionic oxidizing agent into the solution, it gradually diffused into the pyrrole reservoir and then oxopolymerized the pyrrole monomers into polymers. Finally the sphere-like polypyrrole nanostructures were obtained as a consequence of spatially constraining the sphere-like micelles. A similar self-assembly mechanism occurred when cationic surfactant CTAB and oxidizing agent $FeCl_3$ were used, and as a consequence, polypyrrole nanoparticles were also made. However, the system of pyrrol/APS/CTAB in our previous study[27] suggested that a lamellar structure formed between the cations of the CTAB and the anions of the oxidizing agent APS in the aqueous solution, and was attributed to leading the growth of ribbon-like polypyrrole. A similar mechanism occurs in the system of pyrrol/APS/DTAB (see below). Although the precise mechanism of growth of polypyrrole nanorobbins/nanowires does not seem to be fully understood, it is almost certainly related to the lamellar mesostructure of APS/CTAB and APS/DTAB supramolecular assemblies, which will be addressed in more detail in the following sections. Besides, anionic surfactants such as SDS did not serve as the templates to produce these polypyrrole nanostructures, probably because doped polypyrroles contained counterions in the polymer chains. Anionic surfactants would serve as counterions for the polymer chains, and thus permanently disrupt the structure of the sphere-like micelles.

Effects of Monomer and Surfactant Concentrations. Pyrrole monomers are encapsulated into more or less uniform spherical micelles or between periodical lamellar structures driven by the hydrophobic interaction. There should be a saturated monomer concentration at which the micelles can accommodate the maximum number of monomers, because the total interior volume of micelles or lamellae is definite at an equilibrium state once the surfactant concentration remains fixed. On the other hand, it was obvious that the number of micelles, that is the interior volume of micelles, is a function of surfactant concentration. Apparently, the morphology of the resulting polypyrrole is bound to be dependent on both pyrrole monomer and surfactant concentrations. A plot as shown in Figure 2 demonstrates a trend in that the polypyrrole nanostructure varies as a function of both monomer and surfactant concentrations in the system of pyrrole/CTAB/APS.

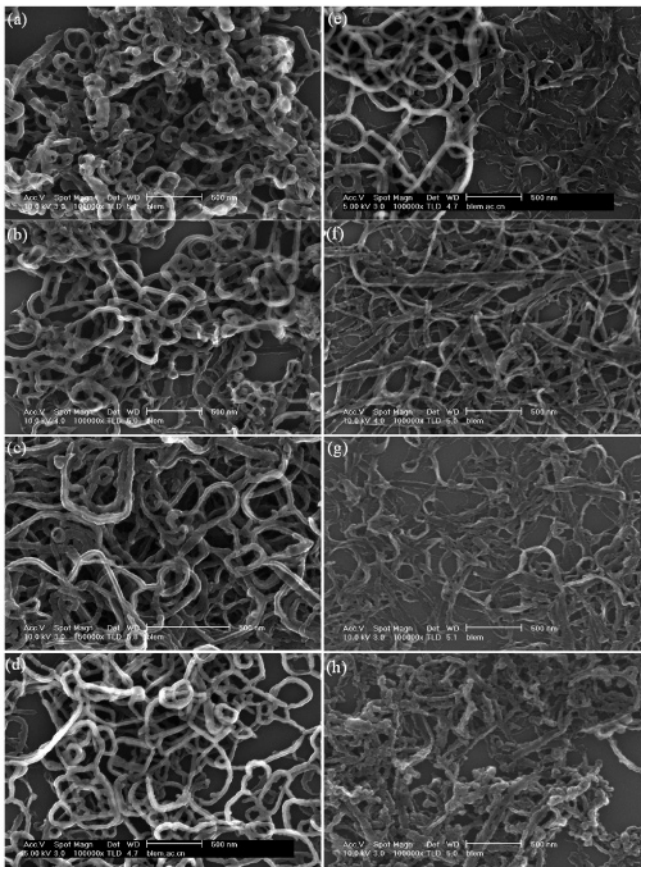

Figure 3. SEM images of polypyrrole nanostructures obtained at different monomer concentrations (CTAB used as a surfactant and its concentration kept the same at 12 cmc, and APS was used as an oxidizing agent): (a) 60, (b) 45, (c) 30, (d) 25, (e) 20, (f) 15, (g) 10, and (h) 5 mM.

First of all, the effect of the monomer concentration on the polypyrrole nanostructure has been revealed and discussed. A series of polymerizations were performed as a function of the monomer concentration from 5 to 60 mM in the systems of CTAB used as a surfactant at a consistent concentration of 12 cmc and APS used as an oxidizing agent. The SEM images of polypyrrole nanostructures are shown in Figure 3 and their corresponding points plotted in Figure 2. It is clearly seen from these two figures that the morphologies of polypyrrole nanostructures change in relation to the concentration of pyrrole monomer. In the condition of the fixed surfactant concentration of 12 cmc, the monomer concentration at 20 mM appeared to be a threshold for determining the resulting polypyrrole nanostructures, below that the polypyrroles were in the form of nanoribbons (Figure 3e−h) and above that in the form of nanowires. The monomer concentration also has a profound influence on the uniformity of the polypyrrole nanostructures. In the experiments, the concentration of 15 mM was also apparent as an optimal monomer concentration for synthesizing polypyrrole nanoribbons in terms of uniformity and yield (Figures 1b and 3f). If the monomer concentration was below 15 mM, the lower the monomer concentration, and the less the resulting polypyrrole uniformity. With the monomer concentration at 10 mM, the relatively uniform ribbonlike polypyrrole nanostructures were still visible (Figure 3g). A further decrease in the monomer concentration to 5 mM resulted in the appearance of protrusions on the edges of polypyrrole nanostructures although the overall morphology remained ribbonlike (Figure 3h), which obviously is ascribed to the shortage of the monomers in some areas between the lamellar mesostructures. Whereas the monomer concentration was increased to or above the threshold 20 mM, wire-like nanostructures of the resulting polypyrrole started to form. For example, when the monomer concentration was kept at 20 mM, the resulting polypyrrole nanostructures resulted in a mixture of the ribbon-like and the wire-like (Figure 2e), which were proved by the TEM observation in our previous work.[27] With a further increase in the monomer concentration from 25 to 45 mM, only wire-like polypyrrole nanostructures were observed (Figure 2d−b). Their diameters were in the range between 20 and 65 nm with lengths up to several micrometers. It seemed that the diameters of the resulting polypyrrole nanowires did not apparently vary, but the nanowires seemed to become more entangled and shorter with increasing monomer concentration. When the monomer concentration was increased to 60 mM, as shown in Figure 2a, some nanowires were entangled or twisted tightly, and some even enclosed themselves into more or less ring-like structures. Excess monomers may account for the above phenomenon. The superfluous pyrrole could not enter into the hydrorphobic layers of the self-assembled mesostructures and thus be oxopolymerized at the exterior of the templates. Similar profiles have been seen in another series of polymerizations as a function of the monomer concentration at a consistent surfactant concentration of 2 cmc, corresponding to the experimental points shown in Figure 2. Therefore it is suggested that the monomer concentration would be controllable below the saturated value for obtaining either nanoribbons or nanowires, otherwise polypyrrole nanostructures would become less uniform or even nonuniform after the reaction.

The formation of the wire-like polypyrrole nanostructure is envisaged to be a result from rolling up the ribbon-like polypyrrole, reminiscent of the mechanism reported in the growth of other wire-like or tube-like nanomaterials.[38−40] Apart from the universal driving force by surface energy minimization, in our experiments, some specific factors may also be taken into account for the occurrence of ribbon-like polypyrrole rolling up into the wire-like polypyrrole. Different from many inorganic nanomaterials that are crystals or single crystals, polypyrrole nanoribbons/nanowires are often amorphous.[27] The polypyrrole long chains tend to entangle together due to the hydrogen bonding and $\pi-\pi$ interaction among themselves. Another important aspect assumes that there would be an evolution of self-assembly of templates during the polymerization of polypyrrole nanoribons/nanowires, from micelles to lamellar mesostructure after oxidizing agent APS is added, simultaneously from lamellae back to micelles again as more APS molecules are further reduced. The late transition would assist the roll-up of the initially growing polypyrrole ribbons between the lamellae. In other words, the templates would take a more active role in the formation of polypyrrole ribbons and wires compared with classic micelle templates. Above all, it is likely to determine the final nanostructure of polypyrrole, either wire-like or ribbon-like, by changing the monomer concentration within a certain range.

After continuing polymerization in different conditions, the clear trend of the influence of the monomer concentration, as well as the surfactant concentration on the polypyrrole nanostructure, emerges in the system of pyrrole/CTAB/APS, as shown in Figure 2. The threshold of the pyrrole concentration for the formation of polypyrrole nanoribbons appears to increase gradually from around 7.5 to 15 mM with increasing CTAB concentration from 2 to 12 cmc, as illustrated in Critical Line 1 in Figure 2. This implies a mild influence of surfactant concentration on the growth of nanoribbon. In the region below

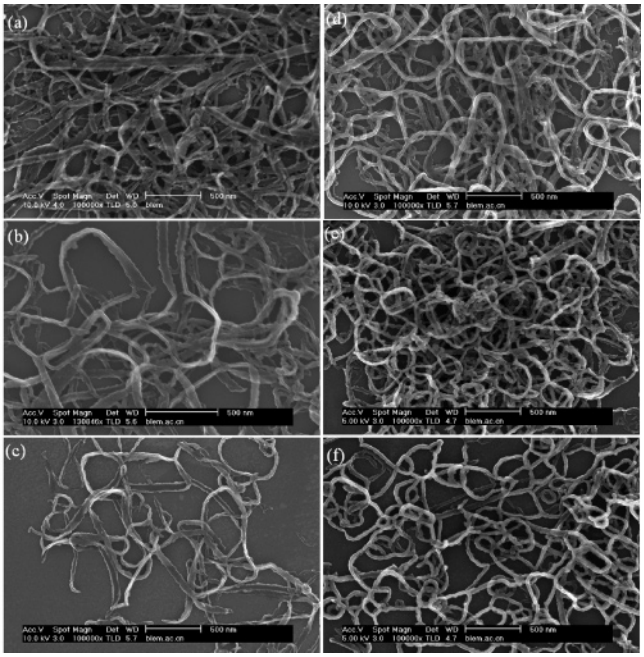

Figure 4. SEM images of polypyrrole nanostructures obtained at different surfactant concentrations (CTAB used as a surfactant and APS used as an oxidizing agent, monomer concentration was kept constant at 15 mM): (a) 12, (b) 10, (c and d) 8, (e) 4, and (f) 2 cmc.

Critical Line 1, polypyrrole nanoribbons are expected. Since the pyrrol concentration in this region is far below the saturated concentration highlighted in Critical Line 2, the micelles would be able to guarantee the uniform dispersion of a small amount of pyrrol monomers, which should be a favored condition for the growth of the nanoribbons. This may help to interpret why the formation of the polypyrrole nanoribbons is more sensitive to the monomer concentration as already demonstrated in Figure 3, rather than the surfactant condition. However, the surfactant concentration is supposed to affect the efficiency and yield of the polymerization, which is still unclear as well. Critical Line 2 illustrates the profile of the saturated pyrrole concentration against the surfactant concentration. The saturated pyrrole concentration for the formation of well-defined polypyrrole nanowires increases more quickly with increasing surfactant concentration in comparison with the threshold concentration in Critical Line 1. It is not surprising that the higher the concentration of the surfactant, the more micelles, and thus the more pyrrole can be well dispersed, remembering that micelle molar concentration $[S_m]$ in equilibrium is given by $[S_m] = K_m[S]^n$, where K_m is the corresponding equilibrium constant, [S] is the molar concentration of the surfactant, and n is the number of surfactant molecules in the micelle, the aggregation number. In the region between Critical Line 1 and Critical Line 2, well-defined polypyrrole nanowire can be synthesized, and moreover, more effective production is anticipated in the condition of higher surfactant and monomer concentrations. Above Critical Line 2, the excess pyrrole outside the templates is involved in the polymerization, and as a result, the morphology of the resulting polypyrrole becomes less uniform and undesirable.

Figure 2 provides a rough guide to the synthesis of polypyrrole with a desired nanostructure in the system of pyrrole/CTAB/APS. For example, when the monomer concentration remained at 15 mM, the nanostructure of the resulting polypyrrole formed in a series of surfactant concentrations as shown in Figure 4, and the corresponding points are plotted in Figure 2. It is clearly seen that the polypyrrole nanostructures obtained in Figure 4 are consistent with what we can anticipate from Figure 2. The pyrrole concentration of 15 mM was found to be the threshold for the growth of polypyrrole nanoribbons when the surfactant concentration was 8 cmc, evidenced by the mixture of nanoribbons and nanowires in Figure 4c,d. In addition, the pyrrole concentration of 15 mM is below Critical Line 2. Just as we expected, when the surfactant was increased to 10 and 12 cmc, more or less uniform ribbonlike polypyrrole nanostructures were obtained (Figure 4a,b). On the other hand, when the surfactant concentration is below 8 cmc while the pyrrole concentration of 15 mM is within Critical Line 1 and Critical Line 2, the resulting polypyrrole nanostructures grew into wire-like nanostructures (Figure 4e,f).

As another example, if the monomer concentration is kept at 30 mM, and the surfactant concentration is varied form 12 to 2 cmc, according to Figure 2, we cannot observe the transformation form ribbon-like to wire-like polypyrrole, but we observe the tendency from the uniform wire-like nanostructures of polypyrrole to entangled and irregular structures of polypyrrole. This interpretation is in good agreement with the experimental observation shown in Figure 5.

In the experiments, it was noted that the sphere-like polypyrrole nanostructures did not show the distinct dependence on the monomer concentration, nor on the surfactant concentration except for the small variations in their diameter when using sphere-like micelles as templates. Being aware of the variation of micelle size and volume with many parameters in the various surfactant systems, we suggest that a systematic study of the dependence of the size distribution of the polypyrrole nanospheres on the monomer and surfactant concentrations and compatibility between pyrrole monomer and surfactant micelle would be worthwhile in the future.

Surfactant Chain-Length Effect. The SEM images in Figure 6 show the resulting polypyrrole nanostructures obtained by using different chain-length quaternary ammonium salts as surfactants. APS was used as oxidizing agent, the monomer concentration was constant at 15 mM, and the surfactant concentration was constant at 12 cmc. It was clearly seen that, in the system of either CTAB or DTAB used as surfactant, ribbon-like polypyrrole was obtained (Figure 6a,b), whereas OTAB as surfactant, sphere-like polypyrrole nanostructures was synthesized (Figure 6c). This indicates that the surfactant chain length may affect the morphologies of the polypyrrole nanostructures. As discussed above, the lamellar mesostructures self-assembled between the cations of the cationic surfactants and the anions of the oxidizing agent APS would serve as the templates for the formation of the ribbonlike polypyrrole nanostructures. However, the system of surfactant OTAB with relatively short alkyl chain and oxidizing agent APS accordingly did not provide the lamellar templates. In the previous study,[27] we observed the white precipitate (lamellar mesostructure) when adding the APS aqueous solution into the CTAB aqueous solution and the lamellar mesostructure was confirmed by XRD spectra. Similarly, the white precipitate was observed as well when the APS aqueous solution was added into the DTAB aqueous solution and the XRD spectra also proved the existence of its lamellar structure. However, when APS aqueous solution was added into the OTAB aqueous solution, no white precipitate was observed, which implies that the cations of OTAB did not interact with the anions of the oxidizing agent APS. In fact, sphere-like micelles formed initially via self-assembly among OTAB molecules themselves still remained, templating the formation of spherical polypyrrole. Similar trends in the phase behavior depending on the alkyl tail length have been reported

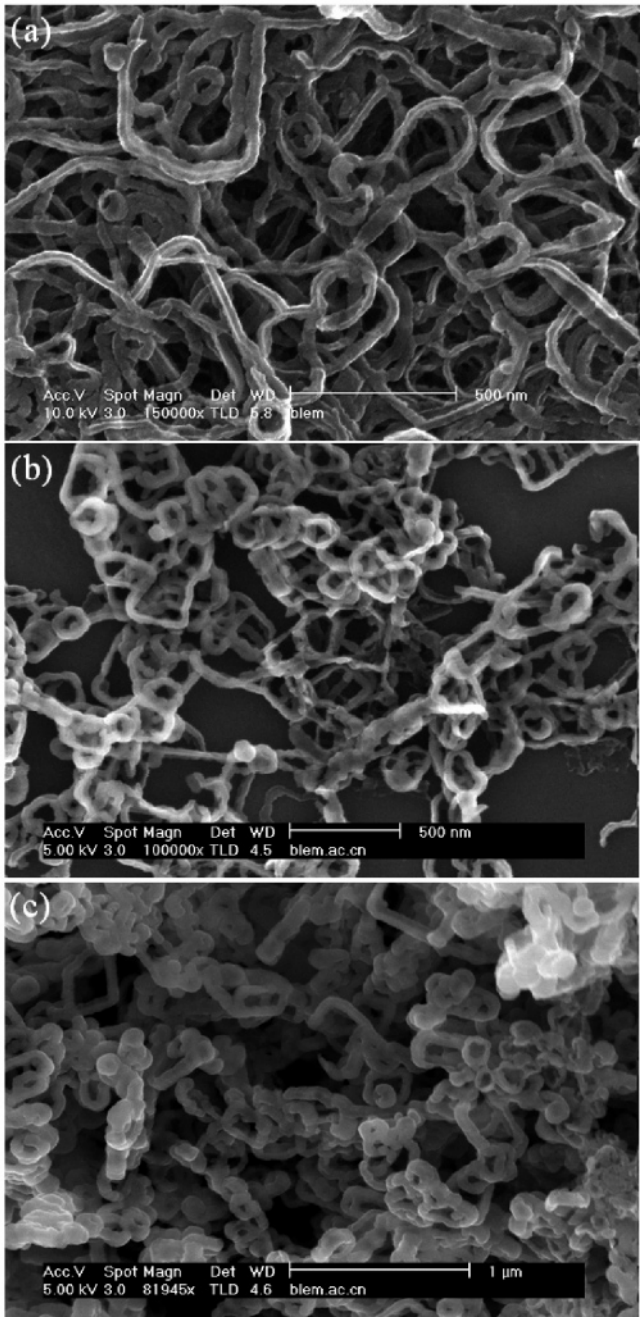

Figure 5. SEM images of polypyrrole nanostructures obtained at different surfactant concentrations (CTAB used as a surfactant and APS used as an oxidizing agent, the monomer concentration was kept constant at 30 mM): (a) 12, (b) 6, and (c) 2 cmc.

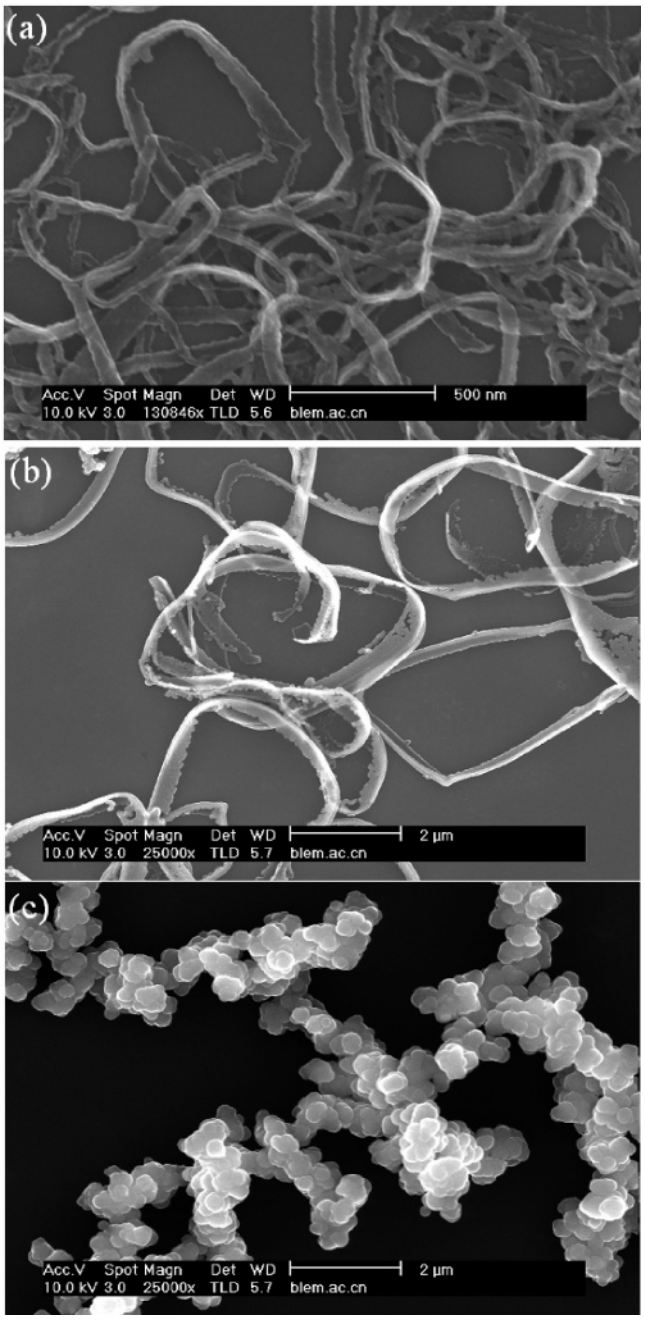

Figure 6. SEM images of polypyrrole nanostructures obtained by using different chain-length quaternary ammonium salts as surfactants (used APS as an oxidizing agent, the monomer concentration was kept constant at 15 mM and the surfactant concentration was kept constant at 12 cmc): (a) CTAB, (b) DTAB, and (c) OTAB.

previously for the mixtures of the same series of cationic surfactant with anionic surfactant.[41,42] The reason for the different assembly behaviors between the long-chain quaternary ammonium salt surfactants, e.g. ,CTAB and DTAB, and the short-chain quaternary ammonium salt surfactants, e.g., OTAB, in the presence of APS is yet to be understood. Nevertheless, these observations indicated that the lamellar mesostructures might be assembled preferentially between the cations of the cationic surfactants with long alkyl chain and the anions of the APS as the templates for synthesis of polypyrrole nanostructures with high aspect ratio.

To rationalize these different assemblies, it is useful to consider the Israelachvilli's packing parameter $P = v/A_0 l_c$, where v is the tail volume, l_c the tail length, and A_0 the area per headgroup.[43] A packing parameter less than $^1/_3$ will yield spherical aggregates, between $^1/_3$ and $^1/_2$ rodlike micelles form, and between $^1/_2$ and 1 bilayers form, and close to 1 planar extended bilayer appears. The pairing of oppositely charged counterions $S_2O_8^{2-}$ from the oxidizing agent APS drastically decreases the headgroup area A_0, thereby increasing the packing parameter P. In fact, when the oxidizing agent was added to the CTAB or DTAB solution, the lamellar white precipitate $(CTA)_2S_2O_8$ could be immediately obtained,[27] from which we could deduce that the planar bilayer of the surfactant aggregates formed first, and then further congregated and deposited from the aqueous solution. So in such a case the electrostatic interactions are strong, and in turn, the packing parameter P would attain values close to 1. For comparison, when SO_4^{2-} was added into the CTAB aqueous solution, we could not see

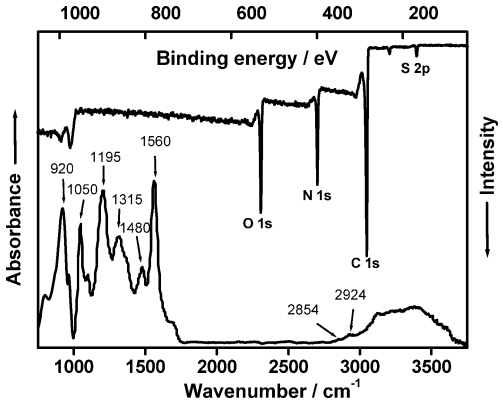

Figure 7. IR spectrum (bottom) and X-ray photoelectron spectrum (top) of the resulting wire-like polypyrrole nanostructures.

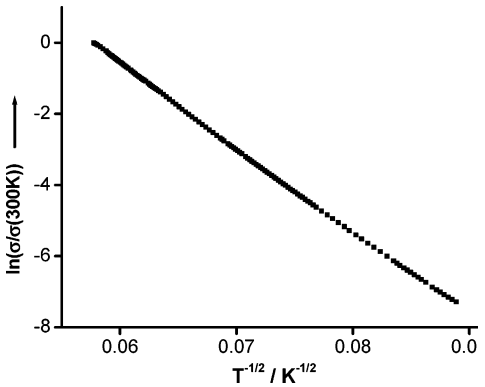

Figure 8. Conductivity−temperature curve of the resulting wire-like polypyrrole.

lamellar precipitates in the presence of SO_4^{2-}, indicating the interactions are not strong enough to induce a bilayer structure or phase separation.[27] Furthermore, for a given headgroup size, the ratio v/l_c is almost unchanged between C_8 and C_{16} chains; however, counterion binding increases with increasing chain length, which results in the decrease of A_0. This may be the reason that increasing the number of carbons in the tails enhances precipitation.

So far, the synthesis methods and the influential parameters have been systematically studied and discussed. In the following paragraphs we will present the characterization and analysis of the resulting polypyrroles. The wire-like polypyrrole nanostructures were chosen as an interesting example.

Composition and Structure. Molecular structures of the resulting wire-like polypyrrole nanostructures obtained by using CTAB as a surfactant and APS as an oxidizing agent were characterized by Fourier transform infrared spectroscopy (FTIR) [Figure 7, bottom]. It was clearly seen that the characteristic polypyrrole peaks are located at 1560 and 1480 cm^{-1}, due to the symmetric and antisymmetric ring-stretching modes, respectively.[44] Strong peaks near 1195 and 920 cm^{-1} indicated the doping state of polypyrrole and a broad band at 3000−3500 cm^{-1} was attributed to N−H and C−H stretching vibrations, respectively.[45,46] Furthermore, the peaks at 1050 and 1315 cm^{-1} were attributed to C−H deformation vibrations and C−N stretching vibrations, respectively.[45,46] The two very weak peaks around 2924 and 2854 cm^{-1} were attributed to the stretching vibration mode of methylene, indicating that surfactants had been almost completely eliminated from the polypyrrole nanostructures. These demonstrated that the resulting polypyrrole nanostructures were pure and in the doping states.

The chemical composition of the wire-like polypyrrole nanostructures was further ascertained by X-ray photoelectron spectroscopy (XPS) [Figure 7, top]. Results indicated that polypyrrole nanostructures were composed of five elements including hydrogen. The elementary composition (mass percent) was [C] 66.64, [N] 15.51, [O] 14.78, and [S] 3.08. The presence of a small amount sulfur indicated that some sulfate anions from reduction of persulfate oxidant had been retained, almost certainly doped into the polypyrrole polymers.[47] The atomic ratio of sulfur ([S]) to nitrogen ([N]) was ∼8.7%, suggesting the presence of one dopant molecule per twelve pyrrole rings. This doping level is far lower than that of one dopant per three pyrrole rings reported.[47] In comparison with the other general synthesis,[48,49] the reasons for such low doping levels are probably ascribed to the following three points: (1) the synthesis occurred in the neutral aqueous solution, (2) the monomer concentration and oxidizing agent concentration were rather low, and (3) the mole ratio of the oxidizing agent to monomer was not very high.

Electrical Properties. Conductivities of the resulting wire-like polypyrrole nanostructures synthesized by using CTAB as a surfactant and APS as an oxidizing agent were measured with the standard Van Der Pauw direct current (DC) four-probe method.[50] Samples used for DC electrical-conductivity measurements were in the form of compressed pellets according to the procedure described in the Experimental Section. The polypyrrole nanostructures showed typical nonmetallic behavior[51] with a conductivity of 7.3×10^{-3} S·cm^{-1} at room temperature (25 °C). The low room temperature conductivity of the polypyrrole nanostructures was ascribed to the low doping level, which had been confirmed by the XPS analysis above. The overall pattern of temperature-dependent conductivity of the polypyrrole nanostructures is well described by Mott's law for quasi-one-dimensional variable-range hopping[52] (Figure 8).

Conclusions

Wire-, ribbon-, and sphere-like polypyrrole nanostructures have been synthesized by the solution chemistry method in the presence of various surfactants (anionic, cationic, or nonionic surfactant) with various oxidizing agents (APS or $FeCl_3$), respectively. Surfactants and oxidizing agents used in this study have played a key role in tailoring the resultant conducting polypyrrole nanostructures. The lamellar mesostructures would be formed by self-assembly between the cations of long chain cationic surfactant (CTAB or DTAB) and anions of the oxidizing agent of APS. These mesostructures have acted as templates for the formation of wire- and ribbon-like polypyrrole nanostructures. While the short chain cationic surfactant OTAB or nonionic surfactant Oπ-10 replaced the long chain cationic surfactant, regardless of oxidizing agent used, sphere-like polypyrrole nanostructures are formed. The surfactants form micelles via self-assembly among surfactant molecules and then serve as the templates. However, when anionic surfactant SDS is used, no polypyrrole nanostructures are obtained as the self-assembly of the surfactant molecules would break down due to the doping effect of anionic surfactants into the resulting polypyrrole chains. The morphologies of the resulting polypyrrole nanostructures are greatly dependent on the monomer concentration, surfactant concentration, and surfactant chain length, which would provide the possibility of elaborate control of the morphologies of the resulting conducting polymers from the sphere-like, to the ribbon-like, to the wire-like. FTIR demonstrates that the resulting polypyrrole nanostructures are pure and in the doped states. XPS analysis suggests the presence of one dopant molecule per twelve pyrrole rings. The overall

profile of temperature-dependent conductivity of the polypyrrole nanostructures is in good agreement with Mott's law for quasi-one-dimensional variable-range hopping with their room temperature conductivity on the order of magnitude −3.

Acknowledgment. This work was supported by National Natural Science Foundation of China (NSFC90206023), Ministry of Science and Technology of China (2001CB6105), and FOKYING TUNG Education Foundation (94012).

References and Notes

(1) Voss, D. *Nature* **2000**, *407*, 442.
(2) Janata, J.; Josowicz, M. *Nature Mater.* **2003**, *2*, 19.
(3) Frank, A. J.; Glenis, S.; Nelson, A. J. *J. Phys. Chem.* **1989**, *93*, 3818.
(4) Argun, A. A.; Cirpan, A.; Reynolds, J. R. *Adv. Mater.* **2003**, *15*, 1338.
(5) Chiu, J. J.; Kei, C. C.; Peng, T. P.; Wang, W. S. *Adv. Mater.* **2003**, *15*, 1361.
(6) Wu, C. G.; Bein, T. *Science* **1994**, *264*, 1757.
(7) Martin, C. R. *Science* **1994**, *266*, 1961.
(8) Carswell, A. D. W.; O'Rear, E. A.; Grady, B. P. *J. Am. Chem. Soc.* **2003**, *125*, 14793.
(9) Hatano, T.; Bae, A. H.; Takeuchi, M.; Fujita, N.; Kaneko, K.; Ihara, H.; Takafuji, M.; Shinkai, S. *Angew. Chem. Int. Ed.* **2004**, *43*, 465.
(10) Fu, M. X.; Zhu, Y. F.; Tan, R. Q.; Shi, G. Q. *Adv. Mater.* **2001**, *13*, 1874.
(11) Tchepournaya, I.; Vasilieva, S.; Logvinov, S.; Timonov, A.; Amadelli, R.; Bartak, D. *Langmuir* **2003**, *19*, 9005.
(12) Jérôme, C.; Demoustier-Champagne, S.; Legras, R.; Jérôme, R. *Chem. Eur. J.* **2000**, *6*, 3089.
(13) Cao, L.; Chen, H. Z.; Zhou, H. B.; Zhu, L.; Sun, J. Z.; Zhang, X. B.; Xu, J. M.; Wang, M. *Adv. Mater.* **2003**, *15*, 909.
(14) Goren, M.; Qi, Z. G.; Lennox, R. B. *Chem. Mater.* **2000**, *12*, 1222.
(15) Dong, H.; Prasad, S.; Nyame, V.; Jones, W. E., Jr. *Chem. Mater.* **2004**, *16*, 371.
(16) Zhang, Z. M.; Wei, Z. X.; Wan, M. X. *Macromolecules* **2002**, *35*, 5937.
(17) Liu, W.; Kumar, J.; Tripathy, S.; Samuelson, L. A. *Langmuir* **2002**, *18*, 9696.
(18) Jang, J.; Oh, J. H. *Chem. Commun.* **2002**, 2200.
(19) Choi, S. J.; Park, S. M. *Adv. Mater.* **2002**, *12*, 1547.
(20) Gorgen, M.; Lennox, R. B. *Nano Lett.* **2001**, *1*, 735.
(21) Hulvat, J. F.; Stupp, S. I. *Angew. Chem. Int. Ed.* **2003**, *42*, 778.
(22) Huang, L. M.; Wang, Z. B.; Wang, H. T.; Cheng, X. L.; Mitra, A.; Yan, Y. S. *J. Mater. Chem.* **2002**, *12*, 388.
(23) Wei, Z. X.; Zhang, L. J.; Yu, M.; Yang, Y. S.; Wan, M. X. *Adv. Mater.* **2003**, *15*, 1382.
(24) Luo, Y. H.; Liu, H. W.; Xi, F.; Li, L.; Jin, X. G.; Han, C. C.; Cha, Z. M. *J. Am. Chem. Soc.* **2003**, *125*, 6447.
(25) Qu, L. T.; Shi, G. Q.; Chen, F. E.; Zhang, J. X. *Macromolecules* **2003**, *36*, 1063.
(26) Qu, L. T.; Shi, G. Q. *Chem. Commun.* **2003**, *2*, 206.
(27) Zhang, X. T.; Zhang, J.; Liu, Z. F.; Roninson, C. *Chem. Commun.* **2004**, 1852.
(28) Furst, E. M.; Pagac, E. S.; Tilton, R. D. *Ind. Eng. Chem. Res.* **1996**, *35*, 1566.
(29) Brinker, C. J.; Lu, Y.; Sellinger, A.; Fan, H. *Adv. Mater.* **1999**, *11*, 579.
(30) Ottaviani, M. F.; Andechaga, P.; Turro, N. J.; Tomalia, D. A. *J. Phys. Chem. B* **1997**, *101*, 6057.
(31) Zielinski, R.; Ikeda, S.; Nomura, H.; Kato, S. *J. Chem. Soc., Faraday Trans. 1* **1988**, *84*, 151.
(32) Turro, N. J.; Kuo, P. L.; Somasundaran, P.; Wong, K. *J. Phys. Chem.* **1986**, *90*, 288.
(33) Burducea, G. *Rom. Rep. Phys.* **2004**, *56*, 87.
(34) Goyal, P. S.; Menon, S. V. G.; Dasannacharya, B. A.; Thiyagarajan, P. *Physica B* **1995**, *213* & *214*, 610.
(35) Choi, K. S.; Lichtenegger, H. C.; Stucky, G. D.; McFarland, E. W. *J. Am. Chem. Soc.* **2002**, *124*, 12402.
(36) Bouchama, F.; Thathagar, M. B.; Rothenberg, G.; Turkenburg, D. H.; Eiser, E. *Langmuir* **2004**, *20*, 477.
(37) Wu, A.; Kolla, H.; Manohar, S. K. *Macromolecules* **2005**, *38*, 7873.
(38) Iijima, S. *Nature* **1991**, *354*, 56.
(39) Ebbesen, T. W.; Ajayan, P. M. *Nature* **1992**, *358*, 16.
(40) Li, Y. D.; Li, X. L.; Deng, Z. X.; Zhou, B. C.; Fan, S. S.; Wang, J. W.; Sun, X. M. *Angew. Chem. Int. Ed.* **2002**, *41*, 333.
(41) Huang, J. B.; Zhao, G. X. *Colloid Polym. Sci.* **1995**, *273*, 1088.
(42) Raghavan, A. R.; Fritz, G.; Kaler, E. W. *Langumuir* **2002**, *18*, 3797.
(43) Patrick, H. N.; Warr, G. G.; Manne, S.; Aksay, I. A. *Langmuir* **1999**, 1685.
(44) Cho, G.; Fung, B. M.; Glatzhofer, D. T.; Lee, J. S.; Shul, Y. G. *Langmuir* **2001**, *17*, 456.
(45) Tian, B.; Zerbi, G. *J. Chem. Phys.* **1990**, *92*, 3886.
(46) Tian, B.; Zerbi, G. *J. Chem. Phys.* **1990**, *92*, 3892.
(47) Joo, J.; Lee, J. K.; Lee, S. Y.; Jang, K. S.; Oh, E. J.; Epstein, A. J. *Macromolecules* **2000**, *33*, 5131.
(48) Hawkins, S. J.; Ratcliffe, N. M. *J. Mater. Chem.* **2000**, *10*, 2057.
(49) Zhang, X.; Manohar, S. K. *J. Am. Chem. Soc.* **2004**, *126*, 12714.
(50) Van Der Pauw, L. T. *Philips Res. Rep.* **1958**, *13*, 1.
(51) Kaiser, A. B. *Adv. Mater.* **2001**, *13*, 927.
(52) Kaiser, A. B. *Rep. Prog. Phys.* **2001**, *64*, 1.